Assessment of Dual-time-point ^18F-fluorodeoxyglucose-Positron Emission Tomography/Computed Tomography Imaging of Malignant Tumors Using Visually and Semiquantitatively : What Kind of Tumors is Useful?

Assessment of Dual-time-point ^{18}F-fluorodeoxyglucose-Positron Emission Tomography/Computed Tomography Imaging of Malignant Tumors Using Visually and Semiquantitatively: What Kind of Tumors is Useful?

HIROTAKA SEURA, TERUE OKAMURA, KOICHI KOYAMA, and YUTAKA MASUOKA

HIROTAKA SEURA, TERUE OKAMURA, KOICHI KOYAMA, and YUTAKA MASUOKA. Assessment of Dual-time-point 18F-fluorodeoxyglucose-Positron Emission Tomography/Computed Tomography Imaging of Malignant Tumors Using Visually and Semiquantitatively: What Kind of Tumors is Useful? *Osaka City Medical Journal*. 2019, 65, 1, 65-76

Osaka City Med. J. Vol. 65, 65-76, 2019

Assessment of Dual-time-point ^{18}F-fluorodeoxyglucose-Positron Emission Tomography/Computed Tomography Imaging of Malignant Tumors Using Visually and Semiquantitatively: What Kind of Tumors is Useful?

Hirotaka Seura[1)], Terue Okamura[1)], Koichi Koyama[2)], and Yutaka Masuoka[3)]

PET center[1)], Osaka Saiseikai Nakatsu Hospital;
Department of Diagnostic and Interventional Radiology[2)], Osaka City University Graduate School of Medicine; and Department of Radiology[3)], Osaka Prefectural Medical Center for Respiratory and Allergic Diseases

Abstract

Background

To retrospectively evaluate the effectiveness of dual-time-point imaging ^{18}F-fluorodeoxyglucose-positron emission tomography/computed tomography in assessing various malignant tumors at our hospital.

Methods

This study included 1153 patients who underwent dual-time-point imaging from November 2009 to October 2011 (702 males, 451 females), including 1211 histopathologically diagnosed malignant lesions. Early and delayed images were acquired at 1 and 2 h after intravenous injection, respectively. Fluorodeoxyglucose-positron emission tomography/computed tomography images were evaluated visually and semiquantitatively.

Results

According to visual analysis, abnormal uptake was detected in 1032 and 1096 lesions among all tumors, and 362 and 416 among 526 small tumors (diameter <3 cm) in early and delayed images, respectively. On delayed images, abnormal uptake was detected in all lesions showing abnormal uptake in early images, and 64 additional lesions among all tumors and 54 additional lesions among small tumors that had not been detected in early images. Tumors detected in delayed images and not in early images included laryngeal, bile duct, pancreatic, uterine cervical and uterine corpus cancers. In semiquantitative analysis, maximum standardized uptake values differed significantly between early and delayed images in both all tumors and small tumors. Retention index, grouped as $>10\%$, $\geqq -10\%$ but $\leqq 10\%$, and $<-10\%$ were 942, 135 and 14 in all tumors, and 320, 86 and 13 in small tumors, respectively.

Received May 25, 2018; accepted January 15, 2019.
Correspondence to: Hirotaka Seura, MD.
PET center, Osaka Saiseikai Nakatsu Hospital,
2-10-39, Shibata, Kita-ku, Osaka 530-0012, Japan
Tel: +81-6-6372-0712; Fax: +81-6-6372-0732
E-mail: hirotakaseura@yahoo.co.jp

Conclusions

Dual-time-point imaging could be effective when fluorodeoxyglucose uptake is not detected in early images, particularly in tumors with diameter <3 cm.

Key Words: Dual-time-point imaging; FDG-PET/CT; Malignancy; Standardized uptake value (SUV)

Introduction

In recent years, ^{18}F-fluorodeoxyglucose (FDG)-positron emission tomography (PET)/computed tomography (CT) has been widely used as a common diagnostic tool for assessing tumor malignancy, determining the clinical stage of tumors, judging therapeutic effects, and detecting recurrence. FDG-PET/CT has been recognized as a useful diagnostic tool for various malignant tumors, but is known to show some limitations. Differentiation between malignant tumors and benign lesions by FDG accumulation alone is known to be difficult, because FDG accumulates in not only malignant tumors, but also benign lesions including benign tumors and inflammatory lesions.

Dual-time-point imaging (DTPI) FDG-PET/CT has recently been recognized as an excellent and simple tool for improving the diagnostic impact of FDG-PET/CT[1-4]. For this method, PET is usually performed twice, at 1 h (as an early image) and approximately 2 h (as a delayed image) after intravenous injection of FDG. Most malignant tumors show gradually increasing FDG uptake as time advances, whereas benign lesions usually show decreased or unchanged FDG uptake[1,4,5]. Using this difference, DTPI offers higher diagnostic utility than standard FDG-PET/CT.

Previous reports, including meta-analyses, have assessed the usefulness of DTPI[1,2,6]. However, no detailed assessments appear to have investigated DTPI for different malignant tumors using the same PET system. Early and delayed images have usually been compared using standard uptake values (SUV)[1,3,6-8], but no investigations have compared visual analyses.

The purpose of this single-institution study was to retrospectively evaluate the effectiveness of DTPI in visually and semiquantitatively assessing malignant tumors, and to investigate what kind of tumor DTPI is best suited to.

Methods

Patients

A total of 1153 consecutive patients on whom DTPI had been performed from November 2009 to October 2011 were investigated (702 males, 451 females; age range, 17-90 years; median, 68 years). Patients were diagnosed histopathologically, and in total were shown to have 1211 malignant lesions. Numbers of malignant lesions found per location are shown in Table 1.

The software of PET reconstruction for our PET/CT scanners was updated in 2012. There were the obvious differences between before and after software updated images in not only visual analysis but also semi-quantitative analysis, therefore the cases after software updated were not included in this study.

This study was approved by the ethics review board of our hospital (institutional review board number: #H28-051) and was performed in accordance with the ethical standards of the 1964 Declaration of Helsinki and its later amendments.

FDG-PET/CT scanning

Images were acquired with a PET/CT single helical scanner (SET-3000BCT/L; Shimadzu, Kyoto,

Table 1. The number of each malignant lesion

	All tumors	Tumors of less than 3 cm
Head and neck	**303**	**176**
Tongue	42	26
Gingiva	23	8
Oral floor	9	7
Nasal and paranasal sinus	9	1
Epipharynx	14	5
Oropharynx	51	20
Hypopharynx	37	17
Larynx	62	50
Thyroid gland	37	31
Ear canal	7	6
Others	12	5
Chest	**314**	**152**
Lung	286	137
Breast	19	14
Others	9	1
Abdomen	**82**	**52**
Liver	11	7
Bile duct	17	10
Gallbladder	5	3
Pancreas	45	28
Others	4	4
Digestive tract	**348**	**90**
Esophagus	87	21
Stomach	83	27
Duodenum	5	2
Colon	172	40
Others	1	0
Hematology	**90**	**31**
Malignant lymphoma	84	29
Multiple myeloma	6	2
Gynecology	**55**	**16**
Uterine cervix	14	6
Uterine corpus	28	10
Ovary	11	0
Others	2	0
Others	**19**	**9**
Prostate	5	2
Others	14	7

Japan) after the patient had fasted for a minimum of 5 h. Patients were administered FDG at 2.7 MBq/kg body weight and scanned at both 60 and 120 min after injection. Both early and delayed emission images covered the body of the patient from the orbits to the upper thighs and were obtained by three-dimensional acquisition using a z-axis 20-cm field of view. Transmission scans were simultaneously obtained using an external source (Cs-137). Table speed was 1 mm/s. Raw emission images were reconstructed using the Fourier rebinning-dynamic row-action maximum likelihood algorithm, and attenuation was corrected by the measured attenuation correction method. FDG was produced by a cyclotron (CYPRIS-HM12; Sumitomo Heavy Industries, Tokyo, Japan). CT was performed after completion of the delayed PET, using the same field of view to reconstruct PET/CT images. CT parameters used were: peak energy, 120 kV; electric current, 60-180 mA according to patient body shape with appropriate radiation exposure; helical pitch, 7 mm; collimation, 7 mm;

thickness, 7 mm. During CT, patients were requested to perform shallow breathing.

Image analysis

1. Image evaluation

All images were retrospectively reviewed by 2 radiologists, both with more than 10 years of experience. Consensus was reached by discussion.

2. Visual analysis

For all malignant tumor lesions visually detected in either early or delayed images, the observed change in FDG uptake was assigned one of three possible labels: increasing; unchanged; or decreasing. This study defined small malignant tumors as lesions ≦3 cm in diameter, because Ohtaka et al reported that using maximum SUV (SUVmax) corrected by a recovery coefficient curve calculated by measuring sphere activity and dividing that activity by true sphere activity was useful in diagnosing lung cancer lesions ≦3 cm in diameter[9]. Referring to the recovery coefficient curve described in the FDG-PET/CT imaging procedure guidelines for cancers (2nd edition)[10], SUV is underestimated in lesions ≦3 cm because the recovery coefficient is <1.0. On the other hand, if the tumor is >3 cm, the recovery coefficient value approaches 1.0 and SUV is considered to be evaluated accurately. We examined the observed changes in FDG uptake not only for all malignant lesions, but also for small malignant lesions alone.

3. Semiquantitative analysis

Semiquantitative analysis was performed using the SUVmax of malignant tumors. All malignant tumors detected in either early or delayed images and with SUVmax that did not exceed the measurable upper limit were analyzed.

The retention index (RI) compares FDG uptake in the early image to FDG uptake in the delayed image and was calculated for each lesion. RI was calculated using the following formula: RI (%) = (SUVmax of delayed image−SUVmax of early image)/SUVmax of early image×100%.

Suitable RI thresholds have been previously reported as −10% and 10%[11,12]. Malignant tumors were therefore divided into 3 groups using the calculated RI: RI <−10%; RI between −10% and 10%; and RI >10%. The same three categories were applied to the small malignant lesions group.

Statistical analysis

Wilcoxon signed-rank test was used to compare SUVmax between early and delayed images. For all analyses, values of $p<0.05$ were considered statistically significant.

Results

Visual analysis

The results of visual analyses for all 1211 malignant lesions, including details of the locations in the early or delayed images, are shown in Table 2.

1. Lesion detection

A total of 1032 lesions (85.2%) and 1096 lesions (90.5%) were detected in early and delayed images, respectively. All lesions detected on early images were also detected on delayed images. Of the 179 lesions (14.8%) not detected on early images, 64 lesions (35.8%) were detected on delayed images. Typical cases with malignant tumors >3 cm in which delayed images were useful for detecting tumors compared to the early image are shown in Figure 1.

Among all lesions, 526 lesions showed a diameter <3 cm. Of these, 362 lesions (68.8%) and 420 lesions (79.8 %) were detected on early and delayed images, respectively. All lesions detected on early

Table 2. The detectability of malignant lesions in the early image and the delayed image on the visual analysis

	All tumors						Tumors of less than 3 cm					
	early(-)			early(+)			early(-)			early(+)		
	delayed(-)		delayed(+)				delayed(-)		delayed(+)			
Malignant lesions	**115**	**(9.5%)**	**64**	**(5.3%)**	**1032**	**(85.2%)**	**106**	**(20.2%)**	**58**	**(11.0%)**	**362**	**(68.8%)**
Head and neck	**49**	**(16.2%)**	**14**	**(4.6%)**	**240**	**(79.2%)**	**47**	**(26.7%)**	**13**	**(7.4%)**	**116**	**(65.9%)**
Tongue	8	(19.0%)	3	(7.1%)	31	(73.8%)	6	(23.1%)	2	(7.7%)	18	(69.2%)
Gingiva	0	(0.0%)	0	(0.0%)	23	(100.0%)	0	(0.0%)	0	(0.0%)	8	(100.0%)
Oral floor	2	(22.2%)	0	(0.0%)	7	(77.8%)	2	(28.6%)	0	(0.0%)	5	(71.4%)
Nasal and paranasal sinus	0	(0.0%)	0	(0.0%)	9	(100.0%)	0	(0.0%)	0	(0.0%)	1	(100.0%)
Epipharynx	0	(0.0%)	0	(0.0%)	14	(100.0%)	0	(0.0%)	0	(0.0%)	5	(100.0%)
Oropharynx	2	(3.9%)	3	(5.9%)	46	(90.2%)	2	(10.0%)	3	(15.0%)	15	(75.0%)
Hypopharynx	4	(10.8%)	1	(2.7%)	32	(86.5%)	4	(23.5%)	1	(5.9%)	12	(70.6%)
Larynx	24	(38.7%)	6	(9.7%)	32	(51.6%)	24	(48.0%)	6	(12.0%)	20	(40.0%)
Thyroid gland	8	(21.6%)	1	(2.7%)	28	(75.7%)	8	(25.8%)	1	(3.2%)	22	(71.0%)
Ear canal	1	(14.3%)	0	(0.0%)	6	(85.7%)	1	(16.7%)	0	(0.0%)	5	(83.3%)
Others	0	(0.0%)	0	(0.0%)	12	(100.0%)	0	(0.0%)	0	(0.0%)	5	(100.0%)
Chest	**9**	**(2.9%)**	**17**	**(5.4%)**	**288**	**(91.7%)**	**9**	**(5.9%)**	**16**	**(10.5%)**	**127**	**(83.6%)**
Lung	6	(2.1%)	17	(5.9%)	263	(92.0%)	6	(4.4%)	16	(11.7%)	115	(83.9%)
Breast	3	(15.8%)	0	(0.0%)	16	(84.2%)	3	(21.4%)	0	(0.0%)	11	(78.6%)
Others	0	(0.0%)	0	(0.0%)	9	(100.0%)	0	(0.0%)	0	(0.0%)	1	(100.0%)
Abdomen	**17**	**(20.7%)**	**11**	**(13.4%)**	**54**	**(65.9%)**	**15**	**(28.8%)**	**9**	**(17.3%)**	**28**	**(53.8%)**
Liver	8	(72.7%)	1	(9.1%)	2	(18.2%)	7	(100.0%)	0	(0.0%)	0	(0.0%)
Bile duct	5	(29.4%)	4	(23.5%)	8	(47.1%)	4	(40.0%)	3	(30.0%)	3	(30.0%)
Gallbladder	2	(40.0%)	0	(0.0%)	3	(60.0%)	2	(66.7%)	0	(0.0%)	1	(33.3%)
Pancreas	1	(2.2%)	4	(8.9%)	40	(88.9%)	1	(3.6%)	4	(14.3%)	23	(82.1%)
Others	1	(25.0%)	2	(50.0%)	1	(25.0%)	1	(25.0%)	2	(50.0%)	1	(25.0%)
Digestive tract	**27**	**(7.8%)**	**9**	**(2.6%)**	**312**	**(89.7%)**	**23**	**(25.6%)**	**9**	**(10.0%)**	**58**	**(64.4%)**
Esophagus	11	(12.6%)	1	(1.1%)	75	(86.2%)	9	(42.9%)	1	(4.8%)	11	(52.4%)
Stomach	12	(14.5%)	6	(7.2%)	65	(78.3%)	10	(37.0%)	6	(22.2%)	11	(40.7%)
Duodenum	1	(20.0%)	0	(0.0%)	4	(80.0%)	1	(50.0%)	0	(0.0%)	1	(50.0%)
Colon	3	(1.7%)	2	(1.2%)	167	(97.1%)	3	(7.5%)	2	(5.0%)	35	(87.5%)
Others	0	(0.0%)	0	(0.0%)	1	(100.0%)	0		0		0	
Hematology	**7**	**(7.8%)**	**5**	**(5.6%)**	**78**	**(86.7%)**	**7**	**(22.6%)**	**4**	**(12.9%)**	**20**	**(64.5%)**
Malignant lymphoma	6	(7.1%)	4	(4.8%)	74	(88.1%)	6	(20.7%)	4	(13.8%)	19	(65.5%)
Multiple myeloma	1	(16.7%)	1	(16.7%)	4	(66.7%)	1	(50.0%)	0	(0.0%)	1	(50.0%)
Gynecology	**3**	**(5.5%)**	**7**	**(12.7%)**	**45**	**(81.8%)**	**2**	**(12.5%)**	**6**	**(37.5%)**	**8**	**(50.0%)**
Uterine cervix	2	(14.3%)	3	(21.4%)	9	(64.3%)	2	(33.3%)	3	(50.0%)	1	(16.7%)
Uterine corpus	0	(0.0%)	3	(10.7%)	25	(89.3%)	0	(0.0%)	3	(30.0%)	7	(70.0%)
Ovary	1	(9.1%)	1	(9.1%)	9	(81.8%)	0		0		0	
Others	0	(0.0%)	0	(0.0%)	2	(100.0%)	0		0		0	
Others	**3**	**(15.8%)**	**1**	**(5.3%)**	**15**	**(78.9%)**	**3**	**(33.3%)**	**1**	**(11.1%)**	**5**	**(55.6%)**
Prostate	0	(0.0%)	0	(0.0%)	5	(100.0%)	0	(0.0%)	0	(0.0%)	2	(100.0%)
Others	3	(21.4%)	1	(7.1%)	10	(71.4%)	3	(42.9%)	1	(14.3%)	3	(42.9%)

early(–), not detected on early image; early(+), detected on early image; delayed(–), not detected on delayed image; and delayed(+), detected on delayed image.

images were also detected on delayed images. Of the 164 lesions (10.2%) not detected on early images, 58 lesions (35.4%) were detected on delayed images.

Most lesions not detected on early images but detected on delayed images showed diameter <3 cm. Typical cases with malignant tumors ≦3 cm in which delayed images were useful for detecting tumors compared to the early image are shown in Figure 2.

2. Lesion detection per location

Lesions detected on neither early nor delayed images were most frequently head and neck cancers (such as laryngeal, oral floor, thyroid, or tongue cancer), abdominal cancers (such as hepatic or gallbladder cancer), breast cancers, and gastric cancers.

Lesions not detected on early images but detected on delayed images were frequently laryngeal cancer, abdominal cancers (such as bile duct or pancreatic cancer), and gynecological cancers (such as uterine cervical or uterine corpus cancer). On very few occasions, these lesions were from a cancer of a digestive organ.

All lesions of gingival, nasal cavity and paranasal sinus cancer, epipharyngeal cancer, and more than 90% of oropharyngeal, lung and colon cancer were detected on both early and delayed images.

Six lesions larger than 3 cm in diameter were not detected on early images, but all these lesions were detected on delayed images. These lesions were tongue, hepatic, bile duct, ovarian, and lung

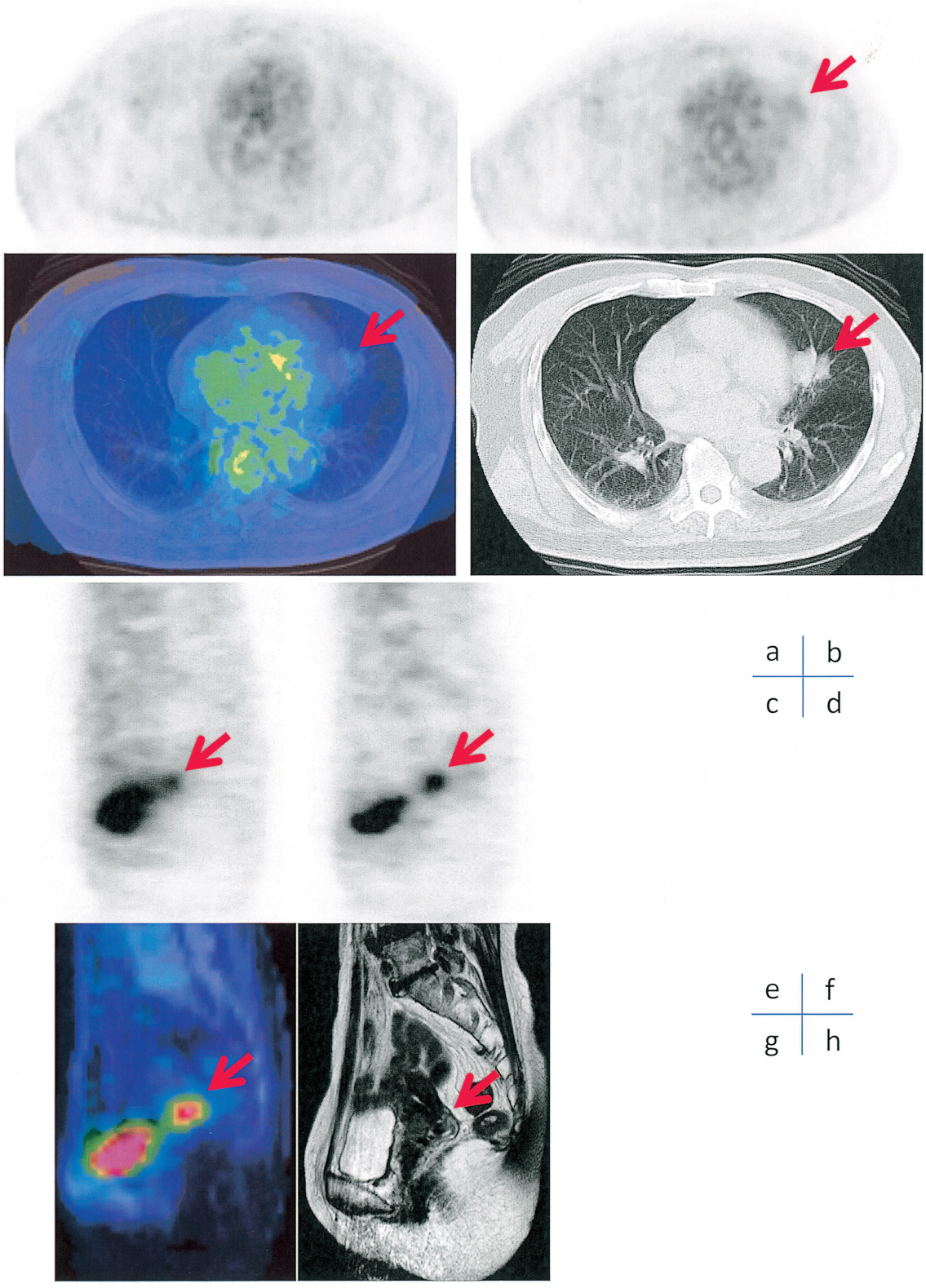

Figure 1. Cancer lesions with diameter ≧3 cm.

a-d) A 67-year-old man with lung cancer (3 cm). The lesion could not be detected on the early image but was detected on the delayed image. a, Early image from FDG-PET (SUVmax 1.2); b, Delayed image from FDG-PET (SUVmax 1.8); c, Delayed image from FDG-PET/CT; and d, CT image.

e-h) A 62-year-old woman with uterine cervical cancer (3.7 cm). The lesion could be detected on both early and delayed images, showing increased FDG uptake on the delayed image. e, Early image from FDG-PET, SUVmax 3.5; f, Delayed image from FDG-PET, SUVmax 4.6; g, Delayed image from FDG-PET/CT; and h, MR image.

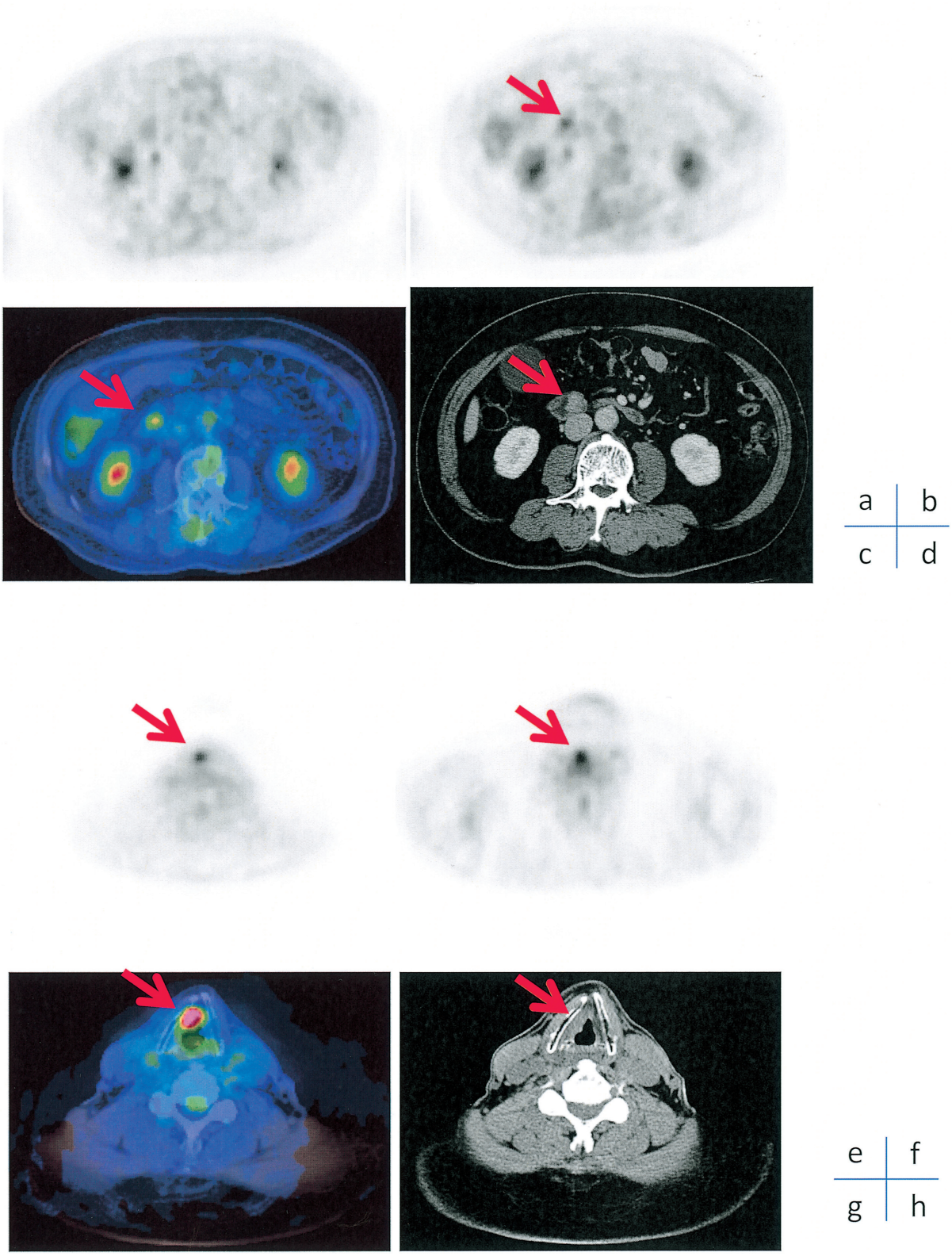

Figure 2. Cancer lesions with diameter <3 cm.

a-d) A 66-year-old man with bile duct cancer. This lesion could not be detected on the early image, but was detectable on the delayed image. a, Early image from FDG-PET (SUVmax 1.8); b, Delayed image from FDG-PET (SUVmax 3.2); c, Delayed image from FDG-PET/CT; and d, CT image.

e-h) A 70-year-old man with laryngeal cancer (1.5 cm), this lesion was detected of both early and delayed images, and showed increasing FDG uptake on delayed image; e, Early image (SUVmax 3.3); f, Delayed image (SUVmax 4.5); g, Delayed image of FDG-PET/CT image; and h, CT image.

cancers, and multiple myeloma.

3. Changes in FDG uptake between early and delayed images

Within head and neck cancers, gingival, epipharyngeal, and oropharyngeal cancers displayed the lowest percentage of lesions that showed increasing FDG uptake. Hypopharyngeal and laryngeal cancers tended to show both increasing and decreasing changes. Other cancers (except hepatic cancer) tended to show increasing FDG uptake. Increasing FDG uptake was observed more frequently in lesions with diameter <3 cm than in all lesions (Table 3).

Semiquantitative analysis

1. SUVmax of all malignant lesions

A total of 1091 lesions were included in this part of the analysis. Because the remaining 120 lesions showed faint or no abnormal uptake, SUVmax of these lesions was too difficult to measure. Mean (±standard deviation) SUVmax was 7.0±5.2 in early images and 8.8±6.4 in delayed images, representing a significant difference ($p<0.0001$).

Among these 1091 lesions, 420 lesions showed diameter <3 cm. For these lesions, SUVmax was 3.8±3.4 in early images and 4.7±4.1 in delayed images, again representing a significant difference ($p<0.0001$).

2. RI of all malignant lesions

Table 3. The changes between FDG uptake in the early images and that in delayed image on the visual analysis

	All tumors				Tumors of less than 3 cm			
	increasing	no change	decreasing	N/A	increasing	no change	decreasing	N/A
Malignant lesions	**751 (68.5%)**	**332 (30.3%)**	**13 (1.2%)**	**115**	**314 (74.8%)**	**94 (22.4%)**	**12 (2.9%)**	**106**
Head and neck	**109 (42.9%)**	**135 (53.1%)**	**10 (3.9%)**	**49**	**67 (51.9%)**	**53 (41.1%)**	**9 (7.0%)**	**47**
Tongue	15 (44.1%)	17 (50.0%)	2 (5.9%)	8	9 (45.0%)	9 (45.0%)	2 (10.0%)	6
Gingiva	5 (21.7%)	18 (78.3%)	0 (0.0%)	0	3 (37.5%)	5 (62.5%)	0 (0.0%)	0
Oral floor	3 (42.9%)	3 (42.9%)	1 (14.3%)	2	2 (40.0%)	2 (40.0%)	1 (20.0%)	2
Nasal and paranasal sinus	7 (77.8%)	2 (22.2%)	0 (0.0%)	0	1 (100.0%)	0 (0.0%)	0 (0.0%)	0
Epipharynx	4 (28.6%)	10 (71.4%)	0 (0.0%)	0	2 (40.0%)	3 (60.0%)	0 (0.0%)	0
Oropharynx	10 (20.4%)	39 (79.6%)	0 (0.0%)	2	5 (27.8%)	13 (72.2%)	0 (0.0%)	2
Hypopharynx	16 (48.5%)	13 (39.4%)	4 (12.1%)	4	8 (61.5%)	2 (15.4%)	3 (23.1%)	4
Larynx	26 (68.4%)	9 (23.7%)	3 (7.9%)	24	19 (73.1%)	4 (15.4%)	3 (11.5%)	24
Thyroid gland	17 (58.6%)	12 (41.4%)	0 (0.0%)	8	14 (60.9%)	9 (39.1%)	0 (0.0%)	8
Ear canal	2 (33.3%)	4 (66.7%)	0 (0.0%)	1	2 (40.0%)	3 (60.0%)	0 (0.0%)	1
Others	4 (33.3%)	8 (66.7%)	0 (0.0%)	0	2 (40.0%)	3 (60.0%)	0 (0.0%)	0
Chest	**266 (87.2%)**	**38 (12.5%)**	**1 (0.3%)**	**9**	**133 (93.0%)**	**9 (6.3%)**	**1 (0.7%)**	**9**
Lung	244 (87.1%)	36 (12.9%)	0 (0.0%)	6	123 (93.9%)	8 (6.1%)	0 (0.0%)	6
Breast	14 (87.5%)	1 (6.3%)	1 (6.3%)	3	9 (81.8%)	1 (9.1%)	1 (9.1%)	3
Others	8 (88.9%)	1 (11.1%)	0 (0.0%)	0	1 (100.0%)	0 (0.0%)	0 (0.0%)	0
Abdomen	**54 (83.1%)**	**11 (16.9%)**	**0 (0.0%)**	**17**	**33 (89.2%)**	**4 (10.8%)**	**0 (0.0%)**	**15**
Liver	1 (33.3%)	2 (66.7%)	0 (0.0%)	8	0	0	0	7
Bile duct	10 (83.3%)	2 (16.7%)	0 (0.0%)	5	6 (100.0%)	0 (0.0%)	0 (0.0%)	4
Gallbladder	2 (66.7%)	1 (33.3%)	0 (0.0%)	2	0 (0.0%)	1 (100.0%)	0 (0.0%)	2
Pancreas	38 (86.4%)	6 (13.6%)	0 (0.0%)	1	24 (88.9%)	3 (11.1%)	0 (0.0%)	1
Others	3 (100.0%)	0 (0.0%)	0 (0.0%)	1	3 (100.0%)	0 (0.0%)	0 (0.0%)	1
Digestive tract	**232 (72.3%)**	**87 (27.1%)**	**2 (0.6%)**	**27**	**50 (74.6%)**	**15 (22.4%)**	**2 (3.0%)**	**23**
Esophagus	48 (63.2%)	27 (35.5%)	1 (1.3%)	11	9 (75.0%)	2 (16.7%)	1 (8.3%)	9
Stomach	53 (74.6%)	17 (23.9%)	1 (1.4%)	12	12 (70.6%)	4 (23.5%)	1 (5.9%)	10
Duodenum	3 (75.0%)	1 (25.0%)	0 (0.0%)	1	1 (100.0%)	0 (0.0%)	0 (0.0%)	1
Colon	127 (75.1%)	42 (24.9%)	0 (0.0%)	3	28 (75.7%)	9 (24.3%)	0 (0.0%)	3
Others	1 (100.0%)	0 (0.0%)	0 (0.0%)	0	0	0	0	0
Hematology	**42 (50.6%)**	**41 (49.4%)**	**0 (0.0%)**	**7**	**14 (58.3%)**	**10 (41.7%)**	**0 (0.0%)**	**7**
Malignant lymphoma	39 (50.0%)	39 (50.0%)	0 (0.0%)	6	13 (56.5%)	10 (43.5%)	0 (0.0%)	6
Multiple myeloma	3 (60.0%)	2 (40.0%)	0 (0.0%)	1	1 (100.0%)	0 (0.0%)	0 (0.0%)	1
Gynecology	**36 (69.2%)**	**16 (30.8%)**	**0 (0.0%)**	**3**	**12 (85.7%)**	**2 (14.3%)**	**0 (0.0%)**	**2**
Uterine cervix	8 (66.7%)	4 (33.3%)	0 (0.0%)	2	3 (75.0%)	1 (25.0%)	0 (0.0%)	2
Uterine corpus	21 (75.0%)	7 (25.0%)	0 (0.0%)	0	9 (90.0%)	1 (10.0%)	0 (0.0%)	0
Ovary	6 (60.0%)	4 (40.0%)	0 (0.0%)	1	0	0	0	0
Others	1 (50.0%)	1 (50.0%)	0 (0.0%)	0	0	0	0	0
Others	**12 (75.0%)**	**4 (25.0%)**	**0 (0.0%)**	**3**	**5 (83.3%)**	**1 (16.7%)**	**0 (0.0%)**	**3**
Prostate	4 (80.0%)	1 (20.0%)	0 (0.0%)	0	1 (50.0%)	1 (50.0%)	0 (0.0%)	0
Others	8 (72.7%)	3 (27.3%)	0 (0.0%)	3	4 (100.0%)	0 (0.0%)	0 (0.0%)	3

Increasing, higher FDG uptake on delayed image than early Image; no change, no significant change between early and delayed image; decreasing, lower FDG uptake on delayed image than on early image; and N/A, not applicable.

A total of 942 lesions (86.3%) showed RI >10%, 135 lesions (12.4%) showed RI between −10% and 10%, and 14 lesions (1.3%) showed RI <−10% (Table 4). Of the 420 lesions with diameter <3 cm, 321 lesions (76.4%) showed RI >10%, 86 lesions (20.5%) showed RI between −10% and 10%, and 13 lesions (3.1%) showed RI <−10% (Table 4).

3. RI per location

Most sites of all tumor lesions and small lesions showed RI >10%, including all nasal cavity and paranasal sinus cancers, hepatic cancers, multiple myelomas, and prostatic cancers. Among cancer lesions with RI between −10% and 10%, the ear canal cancer was the most frequent site (4/6, 66.7%). Fourteen lesions showed RI <−10% in all tumor lesions. These lesions comprised 2 hypopharyngeal cancers, 2 laryngeal cancers, 2 breast cancers, 1 tongue cancer, 1 oropharyngeal cancer, 1 thyroid cancer, 1 lung cancer, 1 esophageal cancer, 1 gastric cancer, 1 colon cancer and 1 malignant lymphoma. Of the 14 lesions above, 13 lesions (excluding 1 case of colon cancer) showed diameter <3 cm (Table 4).

In cases where lesions showed diameter <3 cm, hypopharyngeal and breast cancers frequently showed RI <−10% (Table 4).

Discussion

The utility of DTPI as a diagnostic tool has been reported previously, with most studies focusing

Table 4. Retention index of malignant lesions on the semiquantitative analysis

	All tumors			Tumors of less than 3cm		
	10% < RI	-10% ≤ RI ≤ 10%	RI < -10%	10% < RI	-10% ≤ RI ≤ 10%	RI < -10%
Malignant tumor	**942 (86.3%)**	**135 (12.4%)**	**14 (1.3%)**	**321 (76.4%)**	**86 (20.5%)**	**13 (3.1%)**
Head and neck	**189 (74.4%)**	**58 (22.8%)**	**7 (2.8%)**	**84 (65.1%)**	**38 (29.5%)**	**7 (5.4%)**
Tongue	25 (73.5%)	8 (23.5%)	1 (2.9%)	14 (70.0%)	5 (25.0%)	1 (5.0%)
Gingiva	17 (73.9%)	6 (26.1%)	0 (0.0%)	4 (50.0%)	4 (50.0%)	0 (0.0%)
Oral floor	4 (57.1%)	3 (42.9%)	0 (0.0%)	3 (60.0%)	2 (40.0%)	0 (0.0%)
Nasal and paranasal sinus	9 (100.0%)	0 (0.0%)	0 (0.0%)	1 (100.0%)	0 (0.0%)	0 (0.0%)
Epipharynx	10 (71.4%)	4 (28.6%)	0 (0.0%)	3 (60.0%)	2 (40.0%)	0 (0.0%)
Oropharynx	35 (71.4%)	13 (26.5%)	1 (2.0%)	10 (55.6%)	7 (38.9%)	1 (5.6%)
Hypopharynx	25 (75.8%)	6 (18.2%)	2 (6.1%)	8 (61.5%)	3 (23.1%)	2 (15.4%)
Larynx	31 (81.6%)	5 (13.2%)	2 (5.3%)	20 (76.9%)	4 (15.4%)	2 (7.7%)
Thyroid gland	21 (72.4%)	7 (24.1%)	1 (3.4%)	15 (65.2%)	7 (30.4%)	1 (4.3%)
Ear canal	2 (33.3%)	4 (66.7%)	0 (0.0%)	2 (40.0%)	3 (60.0%)	0 (0.0%)
Others	10 (83.3%)	2 (16.7%)	0 (0.0%)	4 (80.0%)	1 (20.0%)	0 (0.0%)
Chest	**280 (91.8%)**	**22 (7.2%)**	**3 (1.0%)**	**122 (85.3%)**	**18 (12.6%)**	**3 (2.1%)**
Lung	258 (92.1%)	21 (7.5%)	1 (0.4%)	112 (85.5%)	18 (13.7%)	1 (0.8%)
Breast	14 (87.5%)	0 (0.0%)	2 (12.5%)	9 (81.8%)	0 (0.0%)	2 (18.2%)
Others	8 (88.9%)	1 (11.1%)	0 (0.0%)	1 (100.0%)	0 (0.0%)	0 (0.0%)
Abdomen	**53 (81.5%)**	**12 (18.5%)**	**0 (0.0%)**	**27 (73.0%)**	**10 (27.0%)**	**0 (0.0%)**
Liver	3 (100.0%)	0 (0.0%)	0 (0.0%)	0	0	0
Bile duct	10 (83.3%)	2 (16.7%)	0 (0.0%)	4 (66.7%)	2 (33.3%)	0 (0.0%)
Gallbladder	2 (66.7%)	1 (33.3%)	0 (0.0%)	1 (100.0%)	0 (0.0%)	0 (0.0%)
Pancreas	36 (81.8%)	8 (18.2%)	0 (0.0%)	20 (74.1%)	7 (25.9%)	0 (0.0%)
Others	2 (66.7%)	1 (33.3%)	0 (0.0%)	2 (66.7%)	1 (33.3%)	0 (0.0%)
Digestive tract	**294 (91.6%)**	**24 (7.5%)**	**3 (0.9%)**	**56 (83.6%)**	**9 (13.4%)**	**2 (3.0%)**
Esophagus	72 (94.7%)	3 (3.9%)	1 (1.3%)	10 (83.3%)	1 (8.3%)	1 (8.3%)
Stomach	59 (83.1%)	11 (15.5%)	1 (1.4%)	11 (64.7%)	5 (29.4%)	1 (5.9%)
Duodenum	3 (75.0%)	1 (25.0%)	0 (0.0%)	1 (100.0%)	0 (0.0%)	0 (0.0%)
Colon	159 (94.1%)	9 (5.3%)	1 (0.6%)	34 (91.9%)	3 (8.1%)	0 (0.0%)
Others	1 (100.0%)	0 (0.0%)	0 (0.0%)	0	0	0
Hematology	**67 (85.9%)**	**10 (12.8%)**	**1 (1.3%)**	**17 (70.8%)**	**6 (25.0%)**	**1 (4.2%)**
Malignant lymphoma	62 (84.9%)	10 (13.7%)	1 (1.4%)	16 (69.6%)	6 (26.1%)	1 (4.3%)
Multiple myeloma	5 (100.0%)	0 (0.0%)	0 (0.0%)	1 (100.0%)	0 (0.0%)	0 (0.0%)
Gynecology	**44 (84.6%)**	**8 (15.4%)**	**0 (0.0%)**	**9 (64.3%)**	**5 (35.7%)**	**0 (0.0%)**
Uterine cervix	9 (75.0%)	3 (25.0%)	0 (0.0%)	1 (25.0%)	3 (75.0%)	0 (0.0%)
Uterine corpus	24 (85.7%)	4 (14.3%)	0 (0.0%)	8 (80.0%)	2 (20.0%)	0 (0.0%)
Ovary	9 (90.0%)	1 (10.0%)	0 (0.0%)	0	0	0
Others	2 (100.0%)	0 (0.0%)	0 (0.0%)	0	0	0
Others	**15 (93.8%)**	**1 (6.3%)**	**0 (0.0%)**	**6 (100.0%)**	**0 (0.0%)**	**0 (0.0%)**
Prostate	5 (100.0%)	0 (0.0%)	0 (0.0%)	2 (100.0%)	0 (0.0%)	0 (0.0%)
Others	10 (90.9%)	1 (9.1%)	0 (0.0%)	4 (100.0%)	0 (0.0%)	0 (0.0%)

RI, retention index(%).

on the differentiation of malignant and benign tumors[1,4,6,11]. No reports have investigated which malignant tumors benefit most from DTPI, as in the present study. Routine performance of DTPI in all patients has recently been reported as inappropriate[13], as dose exposure is increased for every CT acquisition on the PET/CT scanner. Imaging of the target organ alone is thus becoming more common with DTPI. With the particular PET/CT scanner used in the present study, acquisition of images without unnecessarily increasing the exposure is possible while comparing early and delayed images on an equal basis. We therefore visually and semiquantitatively investigated the kinds of malignant tumor for which DTPI is most useful using only patients scanned at our hospital.

In this study, the detection rate by visual analysis of all malignant tumor lesions was 85.2% on early images and 90.5% on delayed images. This result revealed that delayed images were better than early images for detecting malignant lesions. The detectability of malignant tumor lesions has been reported as 77%-78% on early images and 94% on delayed images, comparable to our results[1,2]. In small lesions <3 cm in diameter, detection rate was 68.8% on early images and 79.8% on delayed images. These detection rates were lower than those corresponding to rates for the group encompassing all lesions. Most lesions not detected on early images showed diameter <3 cm. Only 15 of 685 lesions (2%) with a diameter ≧3 cm were not detected on early images. Of the lesions with diameter <3 cm not detected on early images, approximately one-third were detected on delayed images. DTPI has been reported as useful for small pancreatic cancers, with an average diameter of 2.5 cm[14]. We suppose that DTPI would be useful for lesions with diameters <3 cm.

With regard to the utility of DTPI for different types of tumor, tumor lesions that were difficult to detect on both early and delayed images were more frequently head and neck cancers, abdominal malignant tumors and gastric cancers than other types of tumor lesions. Lesions that could not be detected on early images but were detected on delayed images were only infrequently digestive tract cancers, but were commonly laryngeal cancers, bile duct cancers, pancreatic cancers, uterine cervical cancers, and cancers of the uterine corpus. Most of these tumors showed diameter <3 cm. The utility of DTPI for head and neck cancers has been reported previously[1,15]. However, Yen et al reported that detection rates of epipharyngeal cancer were higher with FDG-PET than with MRI, and no useful additional information was obtained from delayed imaging[16]. Various reports have examined DTPI in thyroid cancer[1,17,18], with limited success, and no reports have examined DTPI for laryngeal cancer. In the present study, while DTPI seemed useful, some laryngeal cancer lesions failed to be detected by FDG accumulation in both early and delayed images, possibly due to tumor disappearance or shrinkage after biopsy. DTPI has already proven useful in detecting bile duct cancer[1,19], and reports have been conflicting regarding differentiation of benign lesions from malignant pancreatic cancers using delayed imaging[20,21]. SUVmax of the pancreatic adenocarcinoma was reported to increase statistically from early to delayed time[22]. In the present study, detecting abnormal FDG uptake on early images was difficult to these lesions due to the nature of the tumors and the small size. DTPI proved useful in detecting both uterine cervical cancer lesions and lesions of the uterine corpus cancer in the present study, but reports are conflicting on the usefulness of DTPI for uterine cervical cancer[23,24] and no reports have examined the situation for cancer of the uterine corpus. In the present study, presence or absence of tumor FDG uptake was determined not only using SUVmax, but also by visually analyzing tumor contrast compared to uptake by surrounding tissue FDG. To the best of our knowledge, no other reports discussing the usefulness of DTPI have investigated tumor FDG uptake in such a manner. Most tumor lesions showed visually increased uptake of FDG. This was attributed

to increased tumor FDG uptake in delayed images and decreased uptake in the surrounding tissue over time. In head and neck cancers, the proportion of lesions showing increasing FDG uptake was small in cases of gingival cancer, epipharyngeal cancer and oropharyngeal cancer among small tumor lesions. In these tumors, the utility of DTPI has been considered limited. Based on the above results, we strongly recommend DTPI as a useful tool for detecting laryngeal cancer, bile duct cancer, pancreatic cancer, uterine cervical cancer, and cancer of the uterine corpus, particularly for small tumors.

In semiquantitative analysis, SUVmax was significantly increased on delayed images compared to early images for both all lesions and lesions smaller than 3 cm. This finding is consistent with results from previous reports[1,2,4].

Concerning RI, 86.3% of all lesions showed RI >10%. For tumors with diameter <3 cm, the three groups of RI >10%, −10%< RI <10% and RI <−10% were almost equivalent to the three groups of increasing, unchanged and decreasing uptake on visual analysis. For all tumors, the group with RI <−10% (1.3%) was almost equivalent to the group with decreasing FDG uptake on visual analysis (1.2%), but the group with RI >10% (86.9%) was larger than the group with increasing FDG uptake on visual analysis (68.9%). This suggests that visually assessing the increase in delayed images is difficult because of the high uptake in large tumors seen even on early images.

Of the only 1.3% of total tumor lesions showing a reduction of >10% in SUVmax, most showed a diameter <3 cm. The hypopharyngeal and breast cancers were included among these lesions. No reports have discussed RI for hypopharyngeal cancer. Our results for the RI of breast cancer were similar to those from other published reports[1].

Within the head and neck cancer group, the proportion of tumor lesions showing increased RI was high among laryngeal, nasal and paranasal cavity cancers. All lesions of the bile duct, pancreatic, uterine cervix and uterine corpus showed increased RI.

The findings of the present study must be considered in light of various limitations. First, this study only analyzed malignant lesions, and benign tumors and inflammatory lesions were not included. Second, since this study was retrospective in design, various biases may have been present despite the inclusion of consecutive patients.

In conclusion, additional delayed imaging appears warranted if tumor FDG uptake cannot be detected on early images, particularly for tumor lesions with diameter <3 cm. Regarding head and neck cancers, DTPI is not thought to be necessary for hypopharyngeal cancer or oral floor cancer, but additional delayed imaging is recommended to be performed for laryngeal cancer. For tumors other than head and neck tumors, additional delayed imaging is recommended to be performed for cancers of the bile duct, pancreas, uterine cervix, and uterine corpus.

Acknowledgments

All authors have no COI to declare regarding the present study.

References

1. Schillaci O. Use of dual-point fluorodeoxyglucose imaging to enhance sensitivity and specificity. Semin Nucl Med 2012;42:267-280.
2. Chan WL, Ramsay SC, Szeto ER, et al. Dual-time-point ^{18}F-FDG-PET/CT imaging in the assessment of suspected malignancy. J Med Imaging Radiat Oncol 2011;55:379-390.
3. Cui J, Zhao P, Ren Z, et al. Evaluation of dual time point imaging 18F-FDG PET/CT in differentiating

malignancy from benign gastric disease. Medicine (Baltimore) 2015;94:e1356.
4. Cheng G, Torigian DA, Zhuang H, et al. When should we recommend use of dual time-point and delayed time-point imaging techniques in FDG PET? Eur J Nucl Med Mol Imaging 2013;40:779-787.
5. Cheng G, Alavi A, Lim E, et al. Dynamic changes of FDG uptake and clearance in normal tissues. Mol Imaging Biol 2013;15:345-352.
6. Saleh Farghaly HR, Mohamed Sayed MH, Nasr HA, et al. Dual time point fluorodeoxyglucose positron emission tomography/computed tomography in differentiation between malignant and benign lesions in cancer patients. Does it always work? Indian J Nucl Med 2015;30:314-319.
7. García Vicente AM, Soriano Castrejón Á, León Martín A, et al. Molecular subtypes of breast cancer: metabolic correlation with ^{18}F-FDG PET/CT. Eur J Nucl Med Mol Imaging 2013;40:1304-1311.
8. Lin WY, Tsai SC, Hung GU. Value of delayed 18F-FDG-PET imaging in the detection of hepatocellular carcinoma. Nucl Med Commun 2005;26:315-321.
9. Ohtaka K, Hida Y, Kaga K, et al. Outcome analysis of (18)F-fluorodeoxyglucose positron-emission tomography in patients with lung cancer after partial volume correction. Anticancer Res 2013;33:5193-5198.
10. Hiroyoshi H, Keiichi O, Takahiro S, et al. Gan FDG-PET/CT satsueihou gaidolain dai2han, Kakuigaku Gijutsu 2013;33:377-420. (In Japanese)
11. Lan XL, Zhang YX, Wu ZJ, et al. The value of dual time point (18)F-FDG PET imaging for the differentiation between malignant and benign lesions. Clin Radiol 2008;63:756-764.
12. Sanz-Viedma S, Torigian DA, Parsons M, et al. Potential clinical utility of dual time point FDG-PET for distinguishing benign from malignant lesions: implications for oncological imaging. Rev Esp Med Nucl 2009; 28:159-166.
13. Lee ST, Scott AM. Are we ready for dual-time point FDG PET imaging? J Med Imaging Radiat Oncol 2011; 55:351-352.
14. Kawada N, Uehara H, Hosoki T, et al. Usefulness of dual-phase 18F-FDG PET/CT for diagnosing small pancreatic tumors. Pancreas 2015;44:655-659.
15. Hustinx R, Smith RJ, Benard F, et al. Dual time point fluorine-18 fluorodeoxyglucose positron emission tomography: a potential method to differentiate malignancy from inflammation and normal tissue in the head and neck. Eur J Nucl Med 1999;26:1345-1348.
16. Yen TC, Chang YC, Chan SC, et al. Are dual-phase ^{18}F-FDG PET scans necessary in nasopharyngeal carcinoma to assess the primary tumour and loco-regional nodes? Eur J Nucl Med Mol Imaging 2005;32:541-548.
17. Lee S, Park T, Park S, et al. The clinical role of dual-time-point ^{18}F-FDG PET/CT in differential diagnosis of the thyroid incidentaloma. Nucl Med Mol Imaging 2014;48:121-129.
18. D'Souza MM, Marwaha RK, Sharma R, et al. Prospective evaluation of solitary thyroid nodule on 18F-FDG PET/CT and high-resolution ultrasonography. Ann Nucl Med 2010;24:345-355.
19. Nishiyama Y, Yamamoto Y, Kimura N, et al. Comparison of early and delayed FDG PET for evaluation of biliary stricture. Nucl Med Commun 2007;28:914-919.
20. Nakamoto Y, Higashi T, Sakahara H, et al. Delayed (18)F-fluoro-2-deoxy-D-glucose positron emission tomography scan for differentiation between malignant and benign lesions in the pancreas. Cancer 2000; 89:2547-2554.
21. Santhosh S, Mittal BR, Bhasin D, et al. Dual-phase 18F-FDG PET/CT imaging in the characterization of pancreatic lesions: does it offer prognostic information? Nucl Med Commun 2014;35:1018-1025.
22. Mena E, Sheikhbahaei S, Taghipour M, et al. 18F-FDG PET/CT metabolic tumor volume and intratumoral heterogeneity in pancreatic adenocarcinomas: impact of dual-time point and segmentation methods. Clin Nucl Med 2017;42:e16-e21.
23. Yen TC, Ng KK, Ma SY, et al. Value of dual-phase 2-fluoro-2-deoxy-d-glucose positron emission tomography in cervical cancer. J Clin Oncol 2003;21:3651-3658.
24. Yu L, Jia C, Wang X, et al. Evaluation of ^{18}F-FDG PET/CT in early-stage cervical carcinoma. Am J Med Sci 2011;341:96-100.